SUPPORTING INFORMATION

Microfluidic Studies of CO_2 Sequestration by Frustrated Lewis Pairs

Dan Voicu[‡□], Milad Abolhasani[*□], Rachelle Choueiri[‡], Gabriella Lestari[‡], Caroline Seiler[‡], Gabriel Menard[‡], Jesse Greener[α], Axel Guenther[*], Douglas W. Stephan[‡], Eugenia Kumacheva[‡σΦ]

[‡] Department of Chemistry, University of Toronto, 80 Saint George Street, Toronto, Ontario M5S 3H6, Canada
[*] Department of Mechanical and Industrial Engineering, University of Toronto, 5 King's College Road, Toronto, Ontario, M5S 3G8, Canada
[α] Départment de Chimie, Université Laval, Pavillon Alexandre-Vachon, local 1220, av. De la Médecine, Québec QC G1V 0A6, Canada
[Φ] Institute of Biomaterials and Biomedical Engineering, University of Toronto, 164 College Street, Toronto, Ontario M5S 3G9, Canada
[σ] Department of Chemical Engineering and Applied Chemistry, University of Toronto, 200 College Street, Toronto, Ontario M5S 3E5, Canada
[□] Authors Contributed Equally

S1. Microfluidic Experimental Setup

The FLP reagents were supplied to the MF reactor using two glass syringes coupled to a syringe pump (PHD2000, Harvard Apparatus). The tubings connected to syringes supplying equal concentrations of tBu$_3$P and Cl(C_6F_5)$_2$ solutions, met at an off-chip T-junction. The solutions were mixed before entering the inlet to the MF reactor. The reactor was purchased from Micronit Microfluidics (R150.332.2). In order to account for reagent dilution upon mixing, each syringe contained a solution of tBu$_3$P or Cl(C_6F_5)$_2$ with the concentration twice as large as the on-chip concentration. For example, to study a 20 mM FLP solution, the syringes were loaded with 40 mM tBu$_3$P and 40 mM Cl(C_6F_5)$_2$ solutions, each, and the individual solutions were supplied to the MF reactor at equal flow rates of 2.5 μL/min. The total on-chip volumetric flow rate of the FLP solution was 5 μL/min. This flow rate was maintained. The CO_2 (Grade 4.0, Linde) gas was supplied from a gas cylinder to the second inlet of the MF reactor via a servo pressure regulator (Marsh Bellofram Type 3000) at P= 118.5 kPa. The reactor was clamped in a custom-made acrylic manifold containing embedded Nanoport connections (IDEX Health Science, USA). Polyether ether ketone tubings with an internal diameter of 0.001" and length of 5' were used to supply reagents and gas to the MF reactor via the Nanoport connections. The FLP solution and CO_2 met at the Y-junction, where they generated alternating gas and liquid segments (Figure S1, inset).

We used 1.25X magnification on an inverted microscope (Olympus Canada) to image segments of CO_2 and FLP solution flowing through the MF reactor and measure the length of the CO_2 plugs. This examined field of view encompassed only a fraction of the MF reactor, as illustrated in Figure S1. We did not analyze the change in the length of CO_2 outside the designated area, which led to the gaps in experimental data points for the reaction time 1.2 - 2 s (Figure 3a).

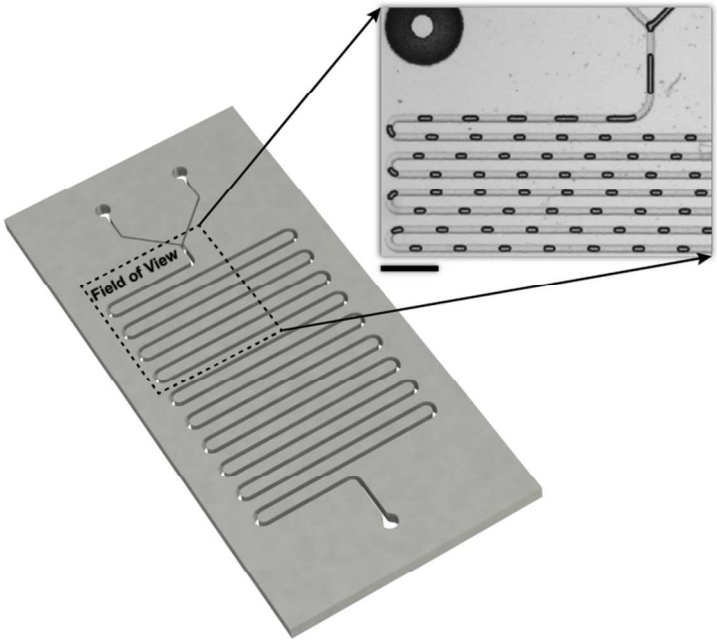

Figure S1. Schematic of the glass MF reactor. The reactor consisted of two inlets that converged at a Y-junction. The field of view used to acquire optical images is shown with a dashed box. The microchannel had the width, height, and length of 150 μm, 150 μm, and 30.4 cm, respectively, and a total volume of 6 μL. The inset shows an optical image of alternating segments of gaseous CO_2 (dark) and the FLP solution (light). Scale bar is 500 μm.

S2. Data Acquisition and Analysis

For each concentration of FLPs, three sequences of 300 images were acquired in the field of view, with at least 4000 bubbles detected. The plug length, L_P, the slug length, L_S, and the velocity of CO_2 plugs, U_P at different microchannel locations, X, were calculated from the images using a Matlab-based program code described elsewhere[1]. The average value of L_p at a particular location was determined and standard deviation was calculated. The Matlab program did not detect plugs flowing through the channel bends, which led to small gaps in the experimental points, e.g., at 0.7 s in Figure 3a.

The average velocity, v, of the CO_2 plugs was calculated in Equation (1) as

$$v = \frac{d_2 - d_1}{t_2 - t_1} \tag{1}$$

where d_1 is the distance of the centre of the plug from the Y-junction at time t_1 and d_2 is the distance of the centre of the plug from the Y-junction one image frame later, at t_2. By using the value of v and the distance-to-time transformation, we determined the reaction time.

The value of L_P was converted to plug volume, V_e, as

$$V_e = H \cdot w\left(L_p - (H - 2d_f)\right) + \pi \cdot \left(w\left(\frac{H}{2} - d_f\right)^2\right) \tag{2}$$

where V_e is the plug volume, H and w are the height and the width of the microchannel, respectively (H= 150 µm, w = 150 µm), and d_f is the thickness of the liquid film surrounding the plug (d_f = 1.5 µm). The volume change of the CO_2 plug was determined by both the physically and chemically mediated shrinkage and the expansion occurring due to the pressure drop along the channel (Figure S2). The experimentally determined plug volume, V_e, depended on both factors. We related the change in CO_2 plug volume in Equation (5).

$$\Delta V_d = \Delta V_e + \Delta V_p \tag{3}$$

where ΔV_d is the change in volume change due to the physical and reaction-induced dissolution of CO_2, ΔV_e is the experimentally determined volume change of the plug, and ΔV_P is the CO_2 plug volume expansion caused by the pressure drop along the channel. We calculated ΔV_p as

$$\Delta V_p = \frac{P_o - P_x}{n_x RT} \tag{4},$$

where P_o is the initial pressure at the Y-junction and P_x is the pressure at distance X from the Y-junction. Although we supplied CO_2 to the MF reactor at pressure 118.5 kPa, the actual pressure at the Y-junction, P_o, was lower, due to the pressure drop along the supplying tubing. The initial pressure at the Y-junction was calculated as

$$P_o = P_{out} + \left(\frac{dP}{dX}\right) L \tag{5},$$

where P_{out} is the atmospheric pressure, dP/dX is the pressure drop along the channel, and L is the total channel length of the microchannel from the Y-junction to the outlet. The pressure drop along the channel was calculated using the correlation proposed by Kreutzer *et al.*[2,3] in Equations (6) and (7) as

$$\frac{\Delta P}{X} = \beta_L f_{slug} \left(\frac{2\rho {U_B}^2}{D_h}\right) \tag{6},$$

$$f_{\text{slug}} = \frac{16}{Re}\left[1 + 0.17\frac{w}{L_{\text{s}}}\left(\frac{Re}{Ca}\right)^{0.33}\right] \quad (7),$$

where $\Delta P/x$ is the pressure drop along the channel, β_{L} is the liquid volume fraction, f_{slug} is the friction factor for segmented flow, Ca is the capillary number, Re is the Reynolds number, and ρ is the liquid density. Using Equation (3), we obtained values of ΔV_{d} from ΔV_{e} and ΔV_{P}.

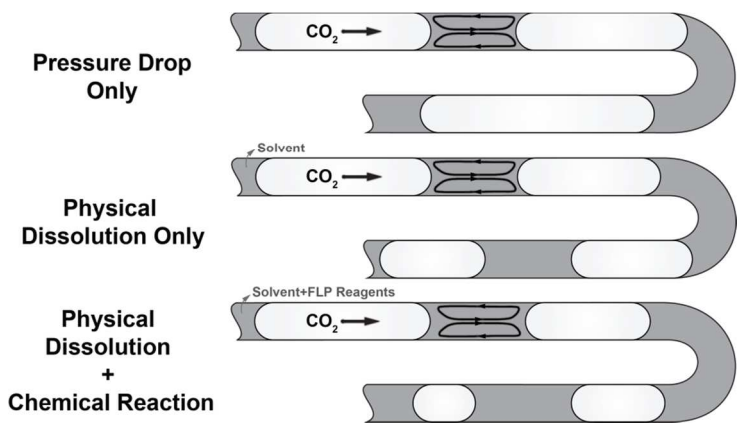

Figure S2. Illustration of the changes in plug volume due to (i) the drop in pressure along the channel, leading to plug expansion, (ii) physical dissolution of CO_2 in the adjacent liquid slug, and (iii) chemical reaction of CO_2 with FLP in the adjacent solution slug. All three effects were present in the FLP-CO_2 system studied in the MF format.

Based on the volume of gaseous plugs, we calculated the number of moles of CO_2 in the plugs at each position along the microchannel using the ideal gas law. With reducing plug length, the number of moles of CO_2 transferred into the adjacent liquid segment was determined as

$$n_{\text{slug(x)}} = n_{\text{(x)}} - n_{\text{o}} \quad (8)$$

where $n_{\text{slug(x)}}$ is the number of moles of CO_2 in the liquid slugs, n_{x} is the number of moles in each gaseous plug at position X, and n_{o} is the initial number of moles of CO_2 in the first plug generated at the Y-junction.

The slug volume, V_{S}, was determined as

$$V_{\text{s}} = H \cdot w \cdot L_{\text{s}} + \left[H \cdot w(H - 2d_{\text{f}}) - \frac{4}{3}\pi\left(\frac{H}{2} - d_{\text{f}}\right)^3\right] \quad (9)$$

We found that the length of the liquid segments did not change with time (Figure S3), which allowed us to assume that the plugs and the slugs moved with the same velocity. Using Equations (10) and (11), we calculated the average

concentration of CO_2 in the liquid slugs, which increased as a result of both the physical dissolution CO_2 in the liquid medium and the reaction-mediated dissolution (the results are presented in Figure 3a for various concentrations of FLP reagents).

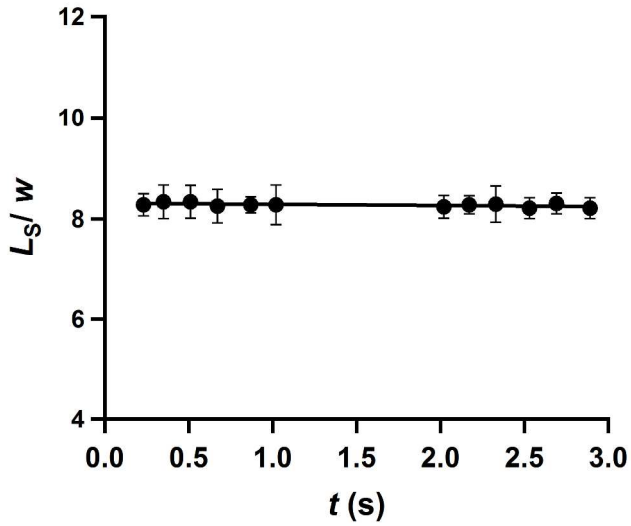

Figure S3. The slug length normalized over channel width, plotted as a function of reaction time.

For the reaction time of 2-3 s, we observed no discernible change in the concentration of CO_2 in the liquid slugs, which indicated that equilibrium was established. To find the reacted CO_2 concentration, C_r, determined by the CO_2-FLP reaction at time t, we subtracted the total CO_2 concentration for the system without FLP, C_{tot}(bromobenzene), from the systems with FLP, C_{tot} (FLP) (Figure 3a).

S3. Micro and Macroscale Physical Dissolution

In this section, we explain the difference in time scales of Figures 2a and 3a in the manuscript, corresponding to the macro- and microscale experiments, respectively. Since the diffusivity, D, of CO_2 within the solvent is the same for both macro- (IR experiment) and microscale experiments, the difference in the time scales results from the difference in diffusion length scales, L_D, of these two experiments:

(a) Macroscale. A stationary 100 μL-volume droplet on the ATR crystal: $L_D \approx 3$ mm.

(b) Microscale. A 6 nL-volume liquid segment entrapped between two CO_2 plugs flowing along the microchannel: $L_D = 37.5$ μm.

In the diffusive processes, time scales as L_D^2. Thus the ratio of the physical dissolution times of CO_2 within the solvent for experiments (a) and (b) can be estimated as

$$\frac{t_{\text{Macro}}}{t_{\text{Micro}}} = \frac{\left[(L_{\text{D}})^2 / D \right]_{\text{Macro}}}{\left[(L_{\text{D}})^2 / D \right]_{\text{Micro}}} = \left[\frac{(L_{\text{D}})_{\text{Macro}}}{(L_{\text{D}})_{\text{Micro}}} \right]^2 = 6400 \tag{10}$$

where t_{Macro} and t_{Micro} are physical dissolution times of CO_2 within the solvent for the IR and MF experiments, respectively.

In order to estimate t_{Micro}, the liquid segment streamline patterns entrapped between two gas plug caps, while flowing in the microchannel are shown in the figure below.

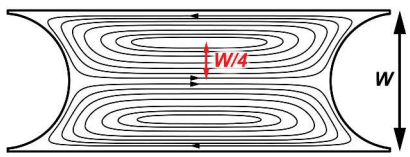

Figure S4. Numerically obtained streamline patterns inside a liquid segment while flowing inside a microchannel.

Due to the convection and symmetric recirculation patterns inside the liquid segment (Figure S4), a quarter of microchannel width, W, can be assumed as the characteristic diffusion length scale in the MF experiment. The diffusion coefficient of CO_2 molecules into bromobenzene, $D_{\text{CO2-BB}}$, is estimated using Versteeg and Swaalj's equation[4,5],

$$D_{\text{CO}_2\text{-BB}} = D_{\text{CO}_2\text{-Water}} \times \left(\frac{\mu_{\text{Water}}(T)}{\mu_{\text{BB}}(T)} \right)^{0.8} \tag{11}$$

where, $D_{\text{CO2-Water}}$ is the diffusion coefficient of CO_2 in water, μ_{Water}(T) and μ_{BB}(T) are viscosities of water and bromobenzene at the temperature T, respectively. Using the estimated $D_{\text{CO2-BB}}$, the physical dissolution time of a 600 μm long boromobenzene segment while flowing in a microchannel with a width of 150 μm can be calculated as:

$$t_{\text{Micro}} = \frac{(W/4)^2}{D_{\text{CO2-BB}}} = 0.85\,\text{s} \tag{12}$$

Thus, in the MF experiment, the physical CO_2 uptake time within the solvent is less than 1 s, while the solvent CO_2 uptake time in the IR experiment would be: $t_{\text{Macro}} = t_{\text{Micro}} \times 6400 = 90.6\,\text{min}$.

S4. Temperature Control for the FLP-CO_2 Reaction

We studied the FLP-CO_2 reaction at 273±2 K, 283±2 K, 293±2 K, 303±2 K, and 313±2 K. To study the reaction at a temperature other than room temperature, 293 K, we submerged the acrylic manifold containing the MF reactor and 3 feet-long supplying tubings in a water bath to allow the FLP solution and CO_2 to reach the desired temperature before entry into the reactor. Figure S5 shows the temperature distribution within the immersed PEEK tubings obtained through a two-dimensional numerical model (COMSOL multiphysics 4.3a) for bromobenzene (a) and CO_2 (b). For increasing liquid flow rate (Figure S5 a), the time of heating or cooling decreases and the required tubing length to reach the target temperature increases. The flow rate used in our work was 5 μL/min, resulting in the requirement for tubing length of 10 mm. The temperature of water in the bath was increased using a bendable heating element (McMasterCarr, Catalog No. 3540K31), which was connected to a digital temperature regulator (Omega, CN8200 series). A type-K thermocouple probe (Sper Scientific, 14003-116) allowed feedback to the temperature controller. To achieve the lower temperatures of 273 K and 283 K, we used a copper heat exchange coil submersed in our water bath coupled to a circulating ethanol-water reservoir pump.

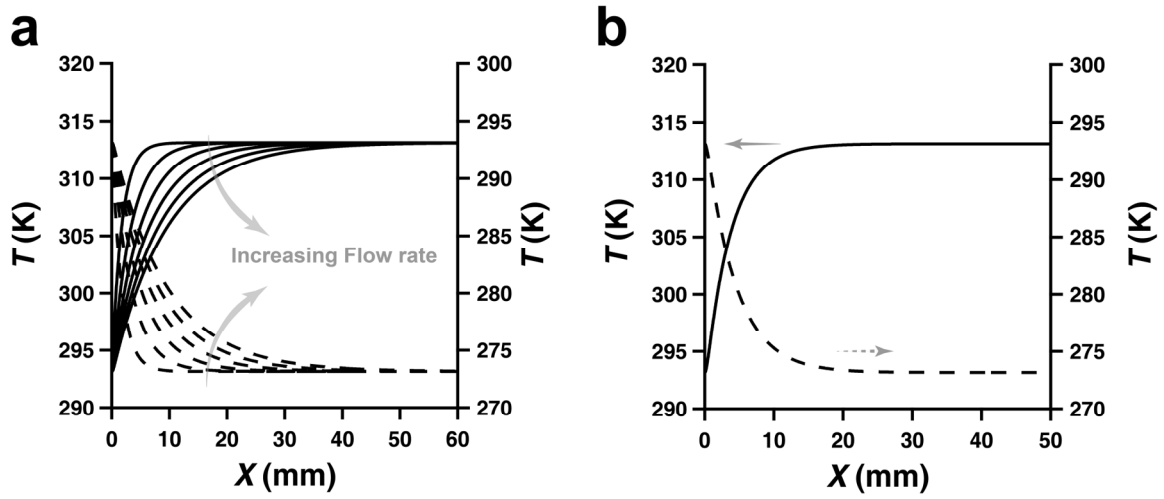

Figure S5. Numerically calculated temperature distribution along PEEK tubing supplying fluids to the MF reactor and immersed into a water bath at a particular temperature. (a) Bromobenzene: heating from 293.15 to 313.15 K (solid lines, left Y-axis); cooling from 293.15 to 273.15 K (dashed lines, right Y-axis). The lowest flow rate was 5 μL/min, the highest flow rate was 30 μL/min (with a 5 μL/min change step). (b) CO_2: heating from 293.15 to 313.15 K (solid line, left Y-axis); cooling from 293.15 to 273.15 K (dashed line, right Y-axis). Inlet pressure was 118.5 kPa.

Since the reaction between FLP reagents and CO_2 is exothermic, there is an expected generation of heat at the gas-liquid interface. This may result in local moderate accumulation of heat (hot spots) in the microchannel immediately downstream of the Y-junction. This heat will be released to the water bath, which maintains the desired

temperature, through conduction via the top and bottom glass surfaces of the MF reactor. Since we are interested in the evaluation of equilibrium constants and the total reaction enthalpy, only the initial and final volumes of CO_2 plugs were considered in our work. According to Figure 3b , the CO_2 plug volume did not change after reaching the equilibrium condition, thereby confirming the constant temperature within the microchannel equal to the water bath temperature, after the equilibrium point.

S5. Infra-Red Spectroscopy Experiments

An attenuated total reflection Fourier transform infrared (ATR-FTIR) spectrometer was used to study physical dissolution of CO_2 in bromobenzene, in solutions of individual reagents in bromobenzene and in a solution of FLPs. A customized home-built gas-tight chamber was placed around the ATR crystal, and purged with dried CO_2 for 10 min. The chamber was then sealed using a rubber membrane and was pressurized with CO_2 at a pressure of 108.2 kPa. A 100 μL-volume droplet of the liquid sample (with a radius of ~3 mm) was placed on the crystal using a syringe that penetrated the rubber membrane of the chamber. The pressure in the chamber was maintained at constant pressure for the duration of the experiment. The variation in intensity of the IR peak at 2343 cm^{-1}, which corresponded to the physically dissolved CO_2 [6] was monitored over the course of 2 hrs. The variation in the peak intensity was studied for bromobenzene, a 80 mM tBu$_3$P solution in bromobenzene, a 80 mM $Cl(C_6F_5)_2$ solution in bromobenzene, and a 160 mM FLP solution in bromobenzene, *vs*. time (Figure 2a). For all four systems we observed the same intensity of the IR peak at 2343 cm^{-1} at equilibrium, suggesting that the solvent properties did not change in the presence of the FLPs or individual reagents, and that the dissolution of CO_2 in bromobenzene could be used as a reference system to study CO_2-FLP reaction.

S6. Validation of the MF methodology

In order to validate a MF approach for the thermodynamic characterization of CO_2-FLP reactions, we examined a well-established and well-characterized reaction between CO_2 and an aqueous solution of diethanolamine (DEA). Using the approach developed for the FLP experiments (described in the main text), we studied the CO_2 mass transfer to the slugs of DEA solutions and obtained information on the equilibrium constants and enthalpy of this reaction. Figure S6 illustrates the volume mass transfer of CO_2 *vs*. distance from the Y-Junction, at 273 K in experiments conducted for four concentrations of DEA in water. Experiments were repeated at 283, 293, and 303 K.

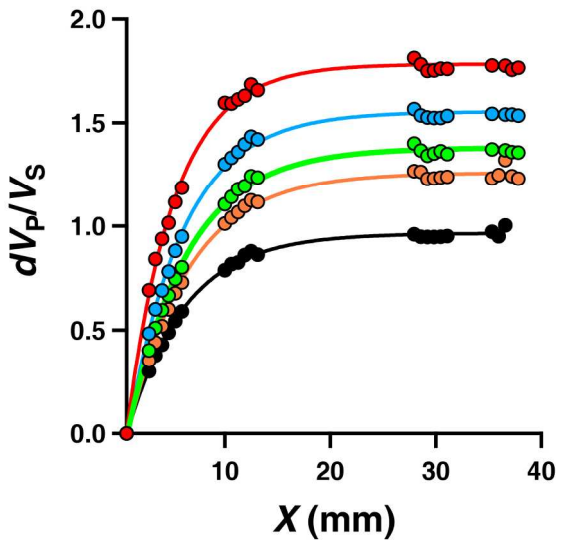

Figure S6. Variation in CO_2 plug shrinkage (normalized by the liquid slug volume (dV_P/V_S), plotted as a function of the distance from the Y-junction at 273 °K. The concentrations of the aqueous DEA solutions are 0 mM (●), 50 mM (●), 75 mM (●), 100 mM (●), and 125 mM (●).The volumetric flow rate of the DEA solution was 6 µL/min, and CO_2 pressure was 119.96 kPa.

Following the method described by Donnellan and Crooks,[7] we calculated an equilibrium constant at each temperature and plotted ln k_{eq} vs. *1/T* to obtain the enthalpy of reaction, as shown in Figure 5 in the main text. The value of ΔH of -69 kJ mol^{-1} obtained for the CO_2-DEA MF experiments compared favorably with the values of ΔH in the range of -67 to -75 kJ mol^{-1}, obtained by the calorimentry, NMR and solubility methods (Table S1).

Table S1. Comparison of the values of ΔH for the CO_2-DEA reaction obtained by different methods

ΔH (kJ mol^{-1})	Method	Reference
-69.4	Microfluidic method	Present work
-72	NMR	8
-69	Irothermal Flow Calorimetry	9
-75	Isoperibol Calorimetry	10
-67	Solubility	11
-69	Isothermal Displacement Calorimetry	12

Movie, CO_2-20 mM FLP. Video of carbon dioxide plugs dissolving into liquid slugs containing 20 mM solution of FLP reagents and bromobenzene. The top left portion of the glass-based MF device is shown here .*Liquid flowrate*= 5 μL/min, *Gas inlet pressure*=118.5 kPa, and *Temperature*=298 K.

References

[1] Abolhasani, M.; Singh, M.; Kumacheva, E.; Guenther, A. *Lab Chip* **2012**, *12*, 1611-1618.

[2] Kreutzer, M. T.; Kapteijn, F.; Moulijn, J. A.; Kleijn, C. R.; Heiszwolf, J. J. *Aiche J.* **2005**, *51*, 2428-2440.;

[3] Kreutzer, M. T.; van der Eijnden, M. G.; Kapteijn, F.; Moulijn, J. A.; Heiszwolf, J. J. *Catal. Today* **2005**, *105*, 667-672.

[4] Versteeg, G.F.; Van Swaaij W.P.M. *Chem. Eng. Sci.* **1988**, 43, 587-591.

[5] Versteeg, G.F.; Van Swaalj W.P.M. *J. Chem. Eng. Data*, **1988**, 33, 29-34.

[6] Falk, M.; Miller, A. G. *Vib. Spectrosc.* **1992**, *4*, 105-108.

[7] Donnellan, J. P.; Crooks, J. E. *J. Chem. Soc. Perkin Trans II* **1989**, 4, 331-333.

[8] Barth, D.; Rubini, P.; Delpuech, J.J. Bull. Soc. Chim. Fr. 1984, 7, 227-230.

[9] Oscarson, J.L.; Van Dam, R.H.; Christensen, J.J.; Izatt, R.M. *Thermochimica Acta* **1989**, 146, 107-114.

[10] Kahrim, A.; Mather, A.E. *Can. J. Chem. Eng.* **1980**, 58, 600-662.

[11] Lee, J.I.; Otto, F.D.; Mather, A.E. *Can J. Chem. Eng.* **1974**, 52, 125-127.

[12] Carson, J.K.; Marsh, K.N. *J. Chem. Theromodynamics* **2000**, 32, 1285-1296.